

# Dark energy and lensing anomaly in Planck CMB data

Ze-Yu Peng<sup>1,2,3,\*</sup> and Yun-Song Piao<sup>1,2,3,4,†</sup>

<sup>1</sup>*School of Physical Sciences, University of Chinese  
Academy of Sciences, Beijing 100049, China*

<sup>2</sup>*International Centre for Theoretical Physics Asia-Pacific,  
University of Chinese Academy of Sciences, 100190 Beijing, China*

<sup>3</sup>*School of Fundamental Physics and Mathematical Sciences,  
Hangzhou Institute for Advanced Study, UCAS, Hangzhou 310024, China*

<sup>4</sup>*Institute of Theoretical Physics, Chinese Academy of Sciences,  
P.O. Box 2735, Beijing 100190, China*

## Abstract

In this paper, we investigate the impact of the lensing anomaly in Planck cosmic microwave background (CMB) data on the nature of dark energy (DE). We constrain the state equation ( $w_0, w_a$ ) of DE with the lensing scaling parameter  $A_L = 1$  and varying  $A_L$ , using the Planck PR3 and two updated Planck PR4 likelihoods, CamSpec and HiLLiPoP respectively, combined with DESI baryon acoustic oscillation (BAO) and Pantheon+ supernova data. As expected, when  $A_L$  is allowed to vary, the evolving DE is not preferred due to the degeneracy between  $w_0, w_a$  and  $A_L$ . In particular, we also consider replacing DESI BAO data with pre-DESI BAO in our analysis, and observe that DESI BAO appears to exacerbate the lensing anomaly, which is caused by the smaller matter density  $\Omega_m$  it prefers, however, this effect can be offset by the shifts in  $w_0$  and  $w_a$  preferring the evolving DE. Our work indicates that the lensing anomaly in Planck data is worth carefully reconsidering when one combined new cosmological survey data with CMB.

---

\* [pengzeyu23@mails.ucas.ac.cn](mailto:pengzeyu23@mails.ucas.ac.cn)

† [yspiao@ucas.ac.cn](mailto:yspiao@ucas.ac.cn)

## I. INTRODUCTION

The Baryon Acoustic Oscillation (BAO) measurements from the first-year observation of Dark Energy Spectroscopic Instrument (DESI), when combined with Cosmic Microwave Background (CMB) and Supernova (SN) data, indicate at  $> 2\sigma$  significance level that dark energy (DE) is evolving [1]. This finding has significant theoretical implications and may profoundly impact our understanding of the nature of DE. There has been extensive discussions and reanalyses of this result [2–34], as well as numerous studies on related theoretical models [35–54]. Furthermore, this  $> 2\sigma$  significance level for evolving DE remains consistent when including the recent DESI full-shape clustering data [55].

It is important to note that the DESI results rely on the Planck 2018 (PR3) CMB data, which dominates the constraints on most cosmological parameter in the analysis. However, the Planck 2018 data are known to exhibit some mild issues, such as the lensing anomaly [56, 57], i.e. the excess lensing effect observed in the CMB power spectra. This anomaly may have non-trivial impacts on the nature for DE due to their degenerate effect. Ref. [32] investigated the evolution of DE in light of lensing anomaly using non-DESI data, see also recent [58].

The last Planck data release (PR4), which employ the NPIPE processing pipeline, is reported with slightly more data, lower noise, and better consistency between frequency channels [59]. Recently updated Planck PR4 likelihoods, including CamSpec [60] and HiLLiPoP [61], both report a weaker lensing anomaly, especially the latter which is consistent with  $A_L = 1$  within  $1\sigma$ . It is also found that these PR4-based likelihoods show better consistency with General Relativity (GR) compared to Planck 2018 [33, 62], and can relax the upper limit on the sum of neutrino masses [63]. Therefore, it is also necessary to revisit the DESI results for evolving DE using these updated Planck likelihoods.

In addition, it is also noteworthy that CMB experiments other than Planck, such as the Atacama Cosmology Telescope (ACT) [64] and the South Pole Telescope (SPT) [65, 66], show no signs of excess lensing effect. A previous study found that that the non-Planck CMB data seem not to prefer the evolving DE [30].

In this paper, we aim to investigate the impact of the lensing anomaly in Planck data on the nature of DE. We constrain the state equation of DE with the lensing scaling parameter  $A_L = 1$  and varying  $A_L$ , using the Planck PR3 and PR4 likelihoods respectively. The paper

is outlined as follows. We describe the methodology and data used in this work in Section II. We present our results on DE with  $A_L = 1$  and varying  $A_L$  for different Planck likelihoods in Section III, and the results with pre-DESI BAO in Section IV. Based on our results, we discuss the underlying physics of the correlation between the evolving DE and the lensing anomaly in Section V. We conclude in Section VI. We also present the results of all relevant parameters in Appendix A.

## II. METHODOLOGY AND DATA

We consider the widely adopted Chevallier-Polarski-Linder (CPL) parameterisation to account for the evolution of DE, in which the DE equation of state is:

$$w(a) = w_0 + w_a(1 - a). \quad (1)$$

We will refer to the corresponding model as  $w_0w_a$ CDM (while  $w_0 = -1$  and  $w_a = 0$  corresponds to  $\Lambda$ CDM), and refer to the models with  $A_L$  varying (so that the lensing spectrum is rescaled as  $C_\ell^{\phi\phi} \rightarrow A_L C_\ell^{\phi\phi}$ ) as  $\Lambda$ CDM+ $A_L$  and  $w_0w_a$ CDM+ $A_L$  respectively.

Tracer	$z_{\text{eff}}$	$D_M/r_d$	$D_H/r_d$	$D_V/r_d$
BGS	0.30	—	—	$7.93 \pm 0.15$
LRG1	0.51	$13.62 \pm 0.25$	$20.98 \pm 0.61$	—
LRG2	0.71	$16.85 \pm 0.32$	$20.08 \pm 0.60$	—
LRG3+ELG1	0.93	$21.71 \pm 0.28$	$17.88 \pm 0.35$	—
ELG2	1.32	$27.79 \pm 0.69$	$13.82 \pm 0.42$	—
QSO	1.49	—	—	$26.07 \pm 0.67$
Lya-QSO	2.33	$39.71 \pm 0.94$	$8.52 \pm 0.17$	—

TABLE I. BAO likelihoods from DESI Year 1 measurements [1].

The Planck CMB PR3 and PR4 likelihoods are described as follows:

- **Plik**: The Planck 2018 (PR3) **Plik** likelihood for high- $\ell$  TT, TE, and EE power spectra, the **Commander** likelihood for low- $\ell$  TT spectrum, and the **SimALL** likelihood for low- $\ell$  EE spectrum [71].

Tracer	$z_{\text{eff}}$	$D_M/r_d$	$D_H/r_d$	$D_V/r_d$
6dF	0.106	—	—	$2.98 \pm 0.13$
MGS	0.15	—	—	$4.47 \pm 0.17$
BOSS Galaxy	0.38	$10.23 \pm 0.17$	$25.00 \pm 0.76$	—
BOSS Galaxy	0.51	$13.36 \pm 0.21$	$22.33 \pm 0.58$	—
eBOSS LRG	0.70	$17.86 \pm 0.33$	$19.33 \pm 0.53$	—
eBOSS ELG	0.85	—	—	$18.33^{+0.57}_{-0.62}$
eBOSS QSO	1.48	$30.69 \pm 0.80$	$13.26 \pm 0.55$	—
eBOSS Lya	2.33	$37.6 \pm 1.9$	$8.93 \pm 0.28$	—
eBOSS Lya-QSO	2.33	$37.3 \pm 1.7$	$9.08 \pm 0.34$	—

TABLE II. BAO likelihoods from pre-DESI measurements, including 6dF Galaxy Survey [67], SDSS DR7 Main Galaxy Sample (MGS) [68], BOSS DR12 Galaxies [69], and eBOSS DR16 [70].

- **CamSpec**: The Planck NPIPE (PR4) CamSpec likelihood for high- $\ell$  TT, TE, and EE power spectra [60], the Commander likelihood for low- $\ell$  TT spectrum, and the SimALL likelihood for low- $\ell$  EE spectrum.
- **HiLLiPoP**: The Planck NPIPE (PR4) HiLLiPoP likelihood for high- $\ell$  TT, TE, and EE power spectra [61], the Commander likelihood for low- $\ell$  TT spectrum, and the NPIPE LoLLiPoP likelihood for low- $\ell$  EE spectrum [72].

These Planck likelihoods are combined with the full DESI BAO likelihoods [1] presented in Table I, where  $z_{\text{eff}}$  is the effective redshift,  $r_d$  is the sound horizon at the drag epoch,  $D_M$  is the comoving distance,  $D_H$  is the Hubble distance, and  $D_V$  is the angle-averaged distance. In Section IV, we also consider replacing DESI BAO with a pre-DESI BAO likelihood, as presented in Table II. For all our analyses, we always include the CMB lensing likelihoods from Planck PR4 [73] and ACT DR6 [74, 75], as well as the Pantheon+ SN Ia data [76].

We perform the Markov chain Monte Carlo (MCMC) analysis using Cobaya [77]. The observables are computed using the cosmological Boltzmann code CLASS [78]. We take our MCMC chains to be converged using the Gelman-Rubin criterion [79] with  $R - 1 < 0.02$ . The best-fit parameters and corresponding  $\chi^2$  values are obtained using PROSPECT, which employs a simulated annealing algorithm<sup>1</sup>. [80]. To quantify the data for the preference of

<sup>1</sup> We use the global optimization method in PROSPECT, which we find is much more effective in finding

models, we calculate the Akaike Information Criterion (AIC) [81] defined as  $AIC = 2k + \chi^2$ , where  $k$  is the number of free parameters in the model.

We adopt wide, uninformative priors for all relevant parameters, including the six standard  $\Lambda$ CDM parameters:  $\ln(10^{10}A_s)$ ,  $n_s$ ,  $H_0$ ,  $\omega_b$ ,  $\omega_{\text{cdm}}$ , and  $\tau_{\text{reio}}$ , the CPL parameters:  $w_0$  and  $w_a$ , and the lensing scaling parameter:  $A_L$ .

### III. RESULTS

Table III presents the marginalized mean and 68% confidence intervals of relevant parameters for  $w_0w_a$ CDM,  $\Lambda$ CDM+ $A_L$ , and  $w_0w_a$ CDM+ $A_L$  with different Planck likelihoods. Table III also presents the  $\Delta\chi^2$  and  $\Delta AIC$  values for each best-fit model relative to the best-fit  $\Lambda$ CDM model using the same dataset. The results of all relevant parameters including the best-fit values are shown in Appendix A.

Fig. 1 displays the posterior distributions of  $w_0 - w_a$  for  $w_0w_a$ CDM (left) and  $w_0w_a$ CDM+ $A_L$  (right). The left panel of Fig. 2 shows the 1D posterior distributions of  $A_L$  for  $\Lambda$ CDM+ $A_L$  (solid) and  $w_0w_a$ CDM+ $A_L$  (dashed), while the right panel shows the scatter plot of  $w_0 - w_a$  for  $w_0w_a$ CDM+ $A_L$  obtained with Plik, with color coding for  $A_L$ .

#### A. Constraints with $A_L = 1$

In this case, we obtain  $w_0 = -0.831 \pm 0.063$  and  $w_a = -0.73_{-0.25}^{+0.29}$  for Plik,  $w_0 = -0.832 \pm 0.063$  and  $w_a = -0.73_{-0.25}^{+0.29}$  for CamSpec, and  $w_0 = -0.842 \pm 0.063$  and  $w_a = -0.64_{-0.24}^{+0.30}$  for HiLLiPoP. As shown in the left panel of Fig. 1, the  $w_0 - w_a$  posterior obtained with CamSpec closely matches that obtained with Plik. The posterior obtained with HiLLiPoP exhibits a slight shift toward the cosmological constant ( $w_0 = -1$ ,  $w_a = 0$ ), but is still consistent with the result with Plik.

The  $\Delta AIC$  values of the best-fit  $w_0w_a$ CDM model relative to  $\Lambda$ CDM are  $-3.56$ ,  $-3.82$ , and  $-1.91$  for Plik, CamSpec, and HiLLiPoP likelihoods, respectively. In view of a goodness-of-fit perspective, we once again find that the CamSpec likelihood maintains the  $> 2\sigma$  significant level for  $w_0w_a$ CDM, while the HiLLiPoP likelihood slightly weakens it, with  $|\Delta AIC| \lesssim 2$ .

---

global minima than the minimizers integrated within Cobaya.

model / dataset	$w_0$	$w_a$	$A_L$	$\Delta\chi^2$	$\Delta\text{AIC}$
<b><math>w_0w_a\text{CDM}</math></b>					
Plik	$-0.831 \pm 0.063$	$-0.73_{-0.25}^{+0.29}$	—	-7.56	-3.56
CamSpec	$-0.832 \pm 0.063$	$-0.73_{-0.25}^{+0.29}$	—	-7.82	-3.82
HiLLiPoP	$-0.842 \pm 0.063$	$-0.64_{-0.24}^{+0.30}$	—	-5.91	-1.91
<b><math>\Lambda\text{CDM}+A_L</math></b>					
Plik	—	—	$1.083_{-0.037}^{+0.033}$	-6.21	-4.21
CamSpec	—	—	$1.075 \pm 0.034$	-4.24	-2.24
HiLLiPoP	—	—	$1.062 \pm 0.035$	-2.63	-0.63
<b><math>w_0w_a\text{CDM}+A_L</math></b>					
Plik	$-0.859 \pm 0.063$	$-0.51_{-0.25}^{+0.32}$	$1.066 \pm 0.041$	-11.26	-5.26
CamSpec	$-0.851 \pm 0.064$	$-0.58_{-0.26}^{+0.32}$	$1.051 \pm 0.040$	-9.41	-3.41
HiLLiPoP	$-0.859 \pm 0.064$	$-0.52_{-0.26}^{+0.30}$	$1.043 \pm 0.040$	-7.73	-1.73

TABLE III. The mean and 68% confidence intervals of relevant parameters for  $w_0w_a\text{CDM}$ ,  $\Lambda\text{CDM}+A_L$ , and  $w_0w_a\text{CDM}+A_L$ , as well as the best-fit  $\Delta\chi^2$  and  $\Delta\text{AIC}$  values relative to  $\Lambda\text{CDM}$ . The datasets used are Planck PR3 and PR4 likelihoods, respectively combined with DESI BAO, CMB lensing, and Pantheon+.

### B. Constraints with varying $A_L$

In this case, we obtain  $w_0 = -0.859 \pm 0.063$  and  $w_a = -0.51_{-0.25}^{+0.32}$  for Plik,  $w_0 = -0.851 \pm 0.064$  and  $w_a = -0.58_{-0.26}^{+0.32}$  for CamSpec, and  $w_0 = -0.859 \pm 0.064$  and  $w_a = -0.52_{-0.26}^{+0.30}$  for HiLLiPoP. As shown in the right panel of Fig. 1, the  $w_0 - w_a$  posteriors of  $w_0w_a\text{CDM}+A_L$  are all consistent with the cosmological constant within  $2\sigma$ . The  $\Delta\text{AIC}$  values of the best-fit  $w_0w_a\text{CDM}+A_L$  model relative to  $\Lambda\text{CDM}+A_L$  are  $-1.05$ ,  $-1.17$ , and  $-1.09$  for Plik, CamSpec, and HiLLiPoP likelihoods, respectively. Therefore, when  $A_L$  is allowed to vary,  $w_0w_a\text{CDM}$  is not preferred.

It is well known that the Planck data has the lensing anomaly in  $\Lambda\text{CDM}+A_L$  model. Here, we have  $A_L = 1.083_{-0.037}^{+0.033}$  for  $\Lambda\text{CDM}+A_L$  with Plik,  $A_L = 1.075 \pm 0.034$  for CamSpec, and  $A_L = 1.062 \pm 0.035$  for HiLLiPoP; while for  $w_0w_a\text{CDM}+A_L$ , we have  $A_L = 1.066 \pm 0.041$  for Plik,  $A_L = 1.051 \pm 0.040$  for CamSpec, and  $A_L = 1.043 \pm 0.040$  for HiLLiPoP. Therefore,

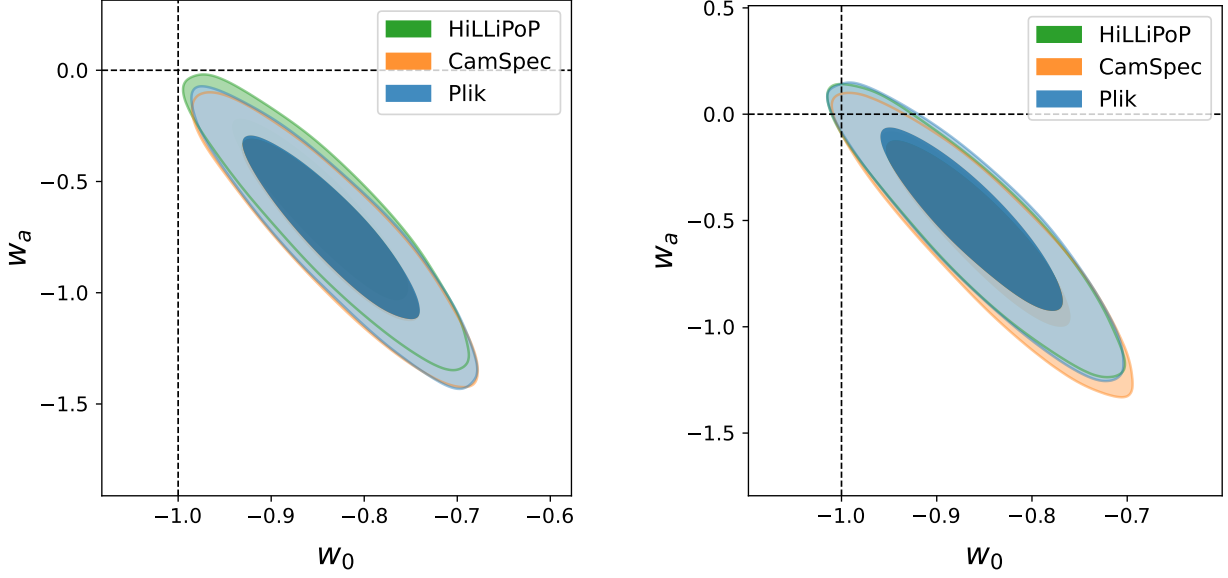


FIG. 1. Posterior distributions (68% and 95% confidence range) of  $w_0 - w_a$  for  $w_0 w_a$ CDM (left) and  $w_0 w_a$ CDM+ $A_L$  (right). The datasets used are Planck PR3 and PR4 likelihoods, respectively combined with DESI BAO, CMB lensing, and Pantheon+.

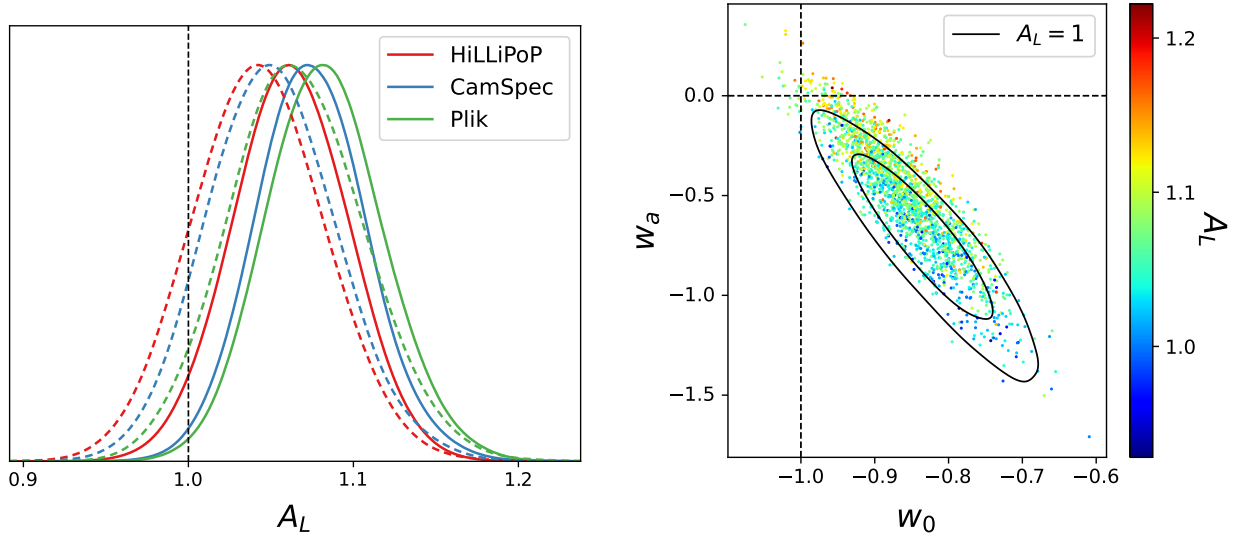


FIG. 2. *Left panel*: 1D posterior distributions of  $A_L$  for  $\Lambda$ CDM+ $A_L$  (solid) and  $w_0 w_a$ CDM+ $A_L$  (dashed). *Right panel*: The scatter plot of  $w_0 - w_a$  for  $w_0 w_a$ CDM+ $A_L$  (obtained with Plik), with color coding for  $A_L$ . The black contour is  $w_0 w_a$ CDM with  $A_L = 1$  for comparison.

the lensing anomaly in Planck data is weakened for  $w_0w_a$ CDM (see also the left panel of Fig. 2). In addition, it is clearly observed from the right panel of Fig. 2 that the  $> 2\sigma$  preference for  $w_0w_a$ CDM is correlated with the abatement of lensing anomaly.

#### IV. COMPARISON WITH PRE-DESI BAO

In this section, to further clarify the effect of DESI BAO on lensing anomaly, we consider replacing DESI BAO with pre-DESI BAO for comparison. Table III presents the marginalized mean and 68% confidence intervals of relevant parameters for  $\Lambda$ CDM+ $A_L$  and  $w_0w_a$ CDM+ $A_L$ . Fig. 3 and Fig. 4 display the 1D and 2D posterior distributions of relevant parameters for  $\Lambda$ CDM+ $A_L$  and  $w_0w_a$ CDM+ $A_L$ , respectively.

model / dataset	$w_0$	$w_a$	$A_L$
<b><math>\Lambda</math>CDM+<math>A_L</math></b>			
Plik	—	—	$1.062 \pm 0.035$
CamSpec	—	—	$1.054 \pm 0.034$
HiLLiPoP	—	—	$1.042 \pm 0.035$
<b><math>w_0w_a</math>CDM+<math>A_L</math></b>			
Plik	$-0.906 \pm 0.062$	$-0.25^{+0.29}_{-0.23}$	$1.067 \pm 0.044$
CamSpec	$-0.902 \pm 0.063$	$-0.30^{+0.29}_{-0.24}$	$1.052 \pm 0.041$
HiLLiPoP	$-0.905 \pm 0.062$	$-0.26^{+0.28}_{-0.23}$	$1.046 \pm 0.042$

TABLE IV. The mean and 68% confidence intervals of relevant parameters for  $\Lambda$ CDM+ $A_L$  and  $w_0w_a$ CDM+ $A_L$ . The datasets are Planck PR3 and PR4 likelihoods, respectively combined with DESI BAO, CMB lensing, and Pantheon+.

The results of  $A_L$  in  $\Lambda$ CDM+ $A_L$  with pre-DESI BAO ( $A_L = 1.062 \pm 0.035$  for Plik,  $A_L = 1.054 \pm 0.034$  for CamSpec, and  $A_L = 1.042 \pm 0.035$  for HiLLiPoP) are smaller than those with DESI BAO, with similar uncertainties. This indicates that DESI BAO slightly exacerbates the lensing anomaly in Planck data.

The results of  $A_L$  with pre-DESI BAO are similar between  $\Lambda$ CDM+ $A_L$  and  $w_0w_a$ CDM+ $A_L$ , which is different from those with DESI BAO. This is related to the fact that pre-DESI BAO itself does not show a preference for evolving DE.



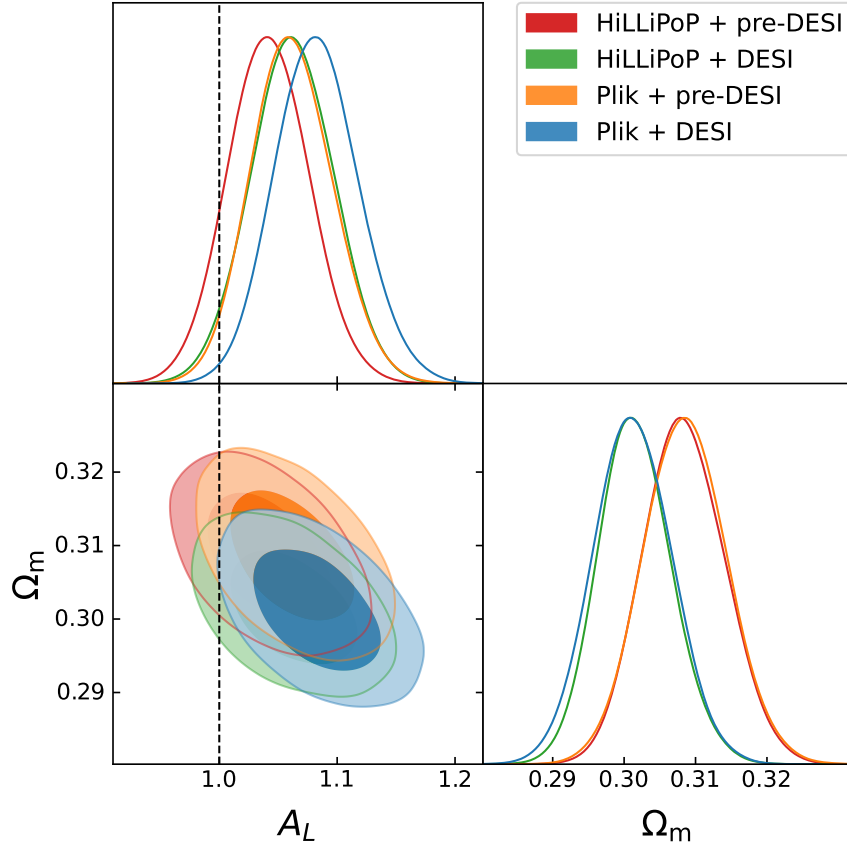


FIG. 3. 1D and 2D marginalized posterior distributions (68% and 95% confidence range) of  $A_L$  and  $\Omega_m$  for  $\Lambda$ CDM+ $A_L$  obtained using Plik and HiLLiPoP, combined with DESI BAO and pre-DESI BAO respectively.

Notably, as shown in Fig. 3, the higher  $A_L$  obtained in  $\Lambda$ CDM+ $A_L$  with DESI BAO is correlated with the smaller  $\Omega_m$  preferred by DESI BAO compared to pre-DESI BAO. This degeneracy exists because a smaller  $\Omega_m$  would suppress the original lensing potential, which should be compensated by a higher  $A_L$ . In the  $w_0w_a$ CDM+ $A_L$  model, we find this degeneracy disappears and there is almost no difference in the  $A_L$  posteriors between DESI BAO and pre-DESI BAO. This is because the effect of smaller  $\Omega_m$  here can be compensated by the shifts in  $w_0$  and  $w_a$ , as seen in Fig. 4.

## V. DISCUSSION ON DE AND LENSING ANOMALY

It is necessary to discuss why the exacerbation of the lensing anomaly in Planck data for  $\Lambda$ CDM, caused by DESI BAO, can be offset by the shifts in  $w_0$  and  $w_a$ . The lensing

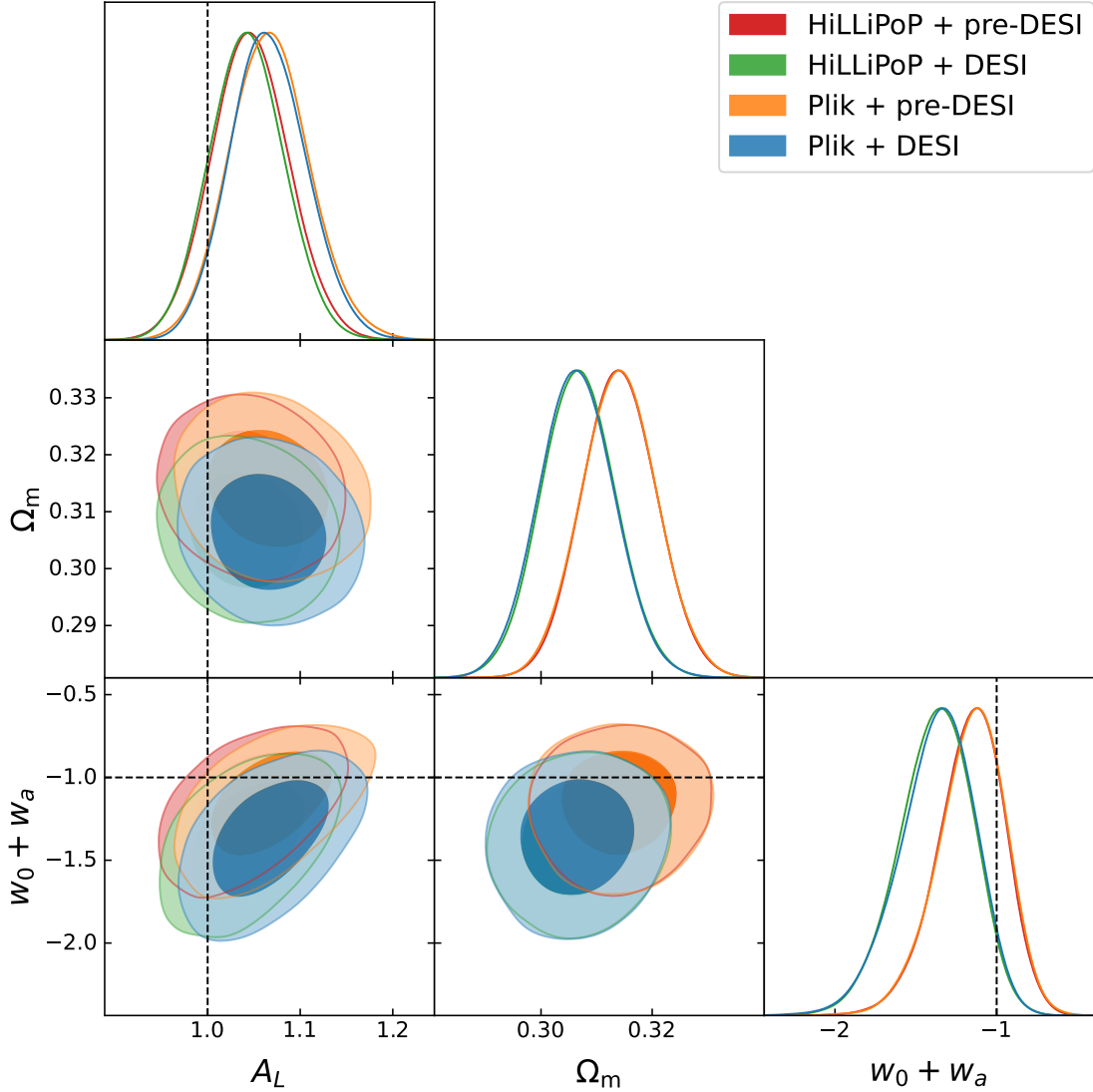


FIG. 4. 1D and 2D marginalized posterior distributions (68% and 95% confidence range) of  $A_L$ ,  $\Omega_m$ , and  $w_0 + w_a$  for  $w_0 w_a \text{CDM} + A_L$ . The datasets are Planck PR4 likelihoods, Plik and HiLLiPoP, combined with DESI BAO and pre-DESI BAO respectively, as well as CMB lensing, and Pantheon+.

potential on the sky (with the comoving distance  $\chi$  to the source), which sets the deflection angle of CMB photons, is given by (in the Newtonian gauge) [82]:

$$\phi_L(\boldsymbol{\theta}) = \int_0^{\chi} \frac{d\chi'}{\chi'} \Phi_W(\mathbf{x}(\boldsymbol{\theta}, \chi')) \left(1 - \frac{\chi'}{\chi}\right), \quad (2)$$

where  $\Phi_W \equiv \Psi + \Phi$  is the Weyl potential. Its evolution in the late universe is determined by the growth function [82]

$$D(a) = \frac{5\Omega_m}{2} \frac{H(a)}{H_0} \int_0^a \frac{da'}{[a'H(a')/H_0]^3}, \quad (3)$$

where  $H(a)/H_0 = \sqrt{\Omega_m a^{-3} + (1 - \Omega_m) a^{-3(1+w(a))}}$  (assuming the universe is flat). Therefore, a lower Hubble expanding rate  $H(a)$  in the past (corresponding to  $w(a) < -1$ ) seems to inevitably magnify the Weyl potential, so the lensing potential, see also e.g. Refs. [83, 84].

We plot the evolution of the Weyl potential in the  $w_0 w_a$ CDM model compared with the  $\Lambda$ CDM model (left) and the corresponding fractional change in the lensing spectrum  $C_\ell^{\phi\phi}$  (right) in Fig. 5. Inspired by the DESI results, we fix  $w_0 = -0.85$  and choose eight different values of  $w_a$  in the range  $[-1.2, 0.2]$ . It can be observed that only the DE models that cross the phantom divide in the past, i.e.  $w_0 + w_a < -1$  preferred by DESI, have the potential to relatively magnify the Weyl potential, and thus suppress the lensing anomaly. We can observe a positive correlation between  $A_L$  and  $w_0 + w_a$  in Fig. 4, especially for the Plik+DESI dataset, and also from the degeneracy direction between  $(w_0, w_a)$  and  $A_L$  in the right panel of Fig. 2.

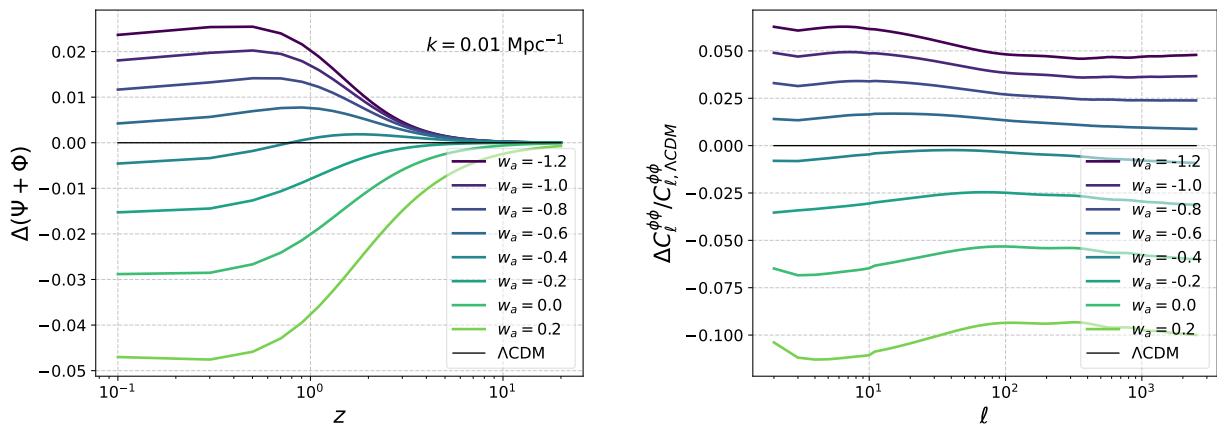


FIG. 5. The evolution of the Weyl potential as a function of redshift in  $w_0 w_a$ CDM models compared with  $\Lambda$ CDM (left), as well as the corresponding fractional change in the lensing spectrum  $C_\ell^{\phi\phi}$  (right). We fix  $w_0 = -0.85$  and choose eight different values of  $w_a$  in the range  $[-1.2, 0.2]$ . All other parameters are fixed to the Planck 2018 best-fit values [71].

## VI. CONCLUSION

In this paper, we investigate the impact of the lensing anomaly in Planck data on the nature of DE, using the Planck PR3 and PR4 likelihoods combined with DESI BAO, CMB lensing and Pantheon+ datasets. The main results are summarized as follows:

- The DESI BAO combined with Pantheon+ and Planck CMB datasets do not prefer the evolution of DE ( $\Lambda$ CDM is  $< 2\sigma$  consistent), when  $A_L$  is allowed to vary<sup>2</sup>.
- The lensing anomaly in the  $\Lambda$ CDM model is exacerbated by DESI BAO, which is caused by the smaller  $\Omega_m$  preferred by DESI BAO, relatively suppressing the lensing potential. However, this effect can be offset by the shifts in  $w_0$  and  $w_a$  preferring the evolving DE.

Therefore, the lensing anomaly in Planck data seems have non-negligible impacts on the nature of DE. In this sense, it is necessary to further explore the potential systematics in updated Planck likelihoods and the implications of the lensing anomaly for DE when one combined new cosmological survey data with CMB.

The nature of DE would also affect our understanding for the very early universe. Though based on the  $\Lambda$ CDM model the Planck collaboration showed the scalar spectral index is  $n_s \approx 0.965$  [85],  $n_s = 1$  ( $n_s - 1 \sim \mathcal{O}(0.001)$ ) is favored [86–91] when the early dark energy (EDE) resolution of Hubble tension is considered<sup>3</sup>, see also [93, 94], and see recent Refs.[95–103] for its implications for inflation models and discussions. It has been observed that with DESI data not only the shift towards  $n_s = 1$  persists, but also the EDE can suppress the preference for evolving DE (making  $\Lambda$ CDM  $< 2\sigma$  consistent) [8]. Thus it can be expected that the results of DESI about DE might be also affected by different solutions to the Hubble tension (see e.g.[104–107]), it will be interesting to revisit relevant results in the light of lensing anomaly.

In all our analyses, we use the Pantheon+ SN Ia data. Notably, DES-Y5 SN data [108], when combined with DESI BAO and CMB data, show stronger significant level ( $> 3\sigma$ ) for evolving DE compared to Pantheon+. Though it has been pointed out in Ref. [109] that

<sup>2</sup> Two PR4-based likelihoods slightly differ in their preferences for the evolving DE when  $A_L = 1$  is fixed, the CamSpec likelihood maintains the  $> 2\sigma$  significant level for evolving DE, while the HiLLiPoP likelihood slightly weakens it.

<sup>3</sup> It seems difficult to ruling out early new physics by using the sound horizon-free measurement of  $H_0$ , e.g.[92].

this preference is likely a result of systematics in the DES-Y5 sample, it is worth exploring the impact of lensing anomaly on the nature of DE using DES-Y5 SN datasets.

## ACKNOWLEDGMENTS

We thank Jun-Qian Jiang, Gen Ye for valuable discussion. This work is supported by NSFC, No.12075246, National Key Research and Development Program of China, No. 2021YFC2203004, and the Fundamental Research Funds for the Central Universities.

- 
- [1] A. G. Adame *et al.* (DESI), (2024), [arXiv:2404.03002 \[astro-ph.CO\]](#).
  - [2] Y. Tada and T. Terada, *Phys. Rev. D* **109**, L121305 (2024), [arXiv:2404.05722 \[astro-ph.CO\]](#).
  - [3] G. Gu, X. Wang, X. Mu, S. Yuan, and G.-B. Zhao, *Res. Astron. Astrophys.* **24**, 065001 (2024), [arXiv:2404.06303 \[astro-ph.CO\]](#).
  - [4] O. Luongo and M. Muccino, (2024), [arXiv:2404.07070 \[astro-ph.CO\]](#).
  - [5] M. Cortês and A. R. Liddle, (2024), [arXiv:2404.08056 \[astro-ph.CO\]](#).
  - [6] E. O. Colgáin, M. G. Dainotti, S. Capozziello, S. Pourojaghi, M. M. Sheikh-Jabbari, and D. Stojkovic, (2024), [arXiv:2404.08633 \[astro-ph.CO\]](#).
  - [7] Y. Carloni, O. Luongo, and M. Muccino, (2024), [arXiv:2404.12068 \[astro-ph.CO\]](#).
  - [8] H. Wang and Y.-S. Piao, (2024), [arXiv:2404.18579 \[astro-ph.CO\]](#).
  - [9] C.-G. Park, J. de Cruz Pérez, and B. Ratra, *Phys. Rev. D* **110**, 123533 (2024), [arXiv:2405.00502 \[astro-ph.CO\]](#).
  - [10] C.-G. Park, J. de Cruz Perez, and B. Ratra, (2024), [arXiv:2405.00502 \[astro-ph.CO\]](#).
  - [11] Z. Wang, S. Lin, Z. Ding, and B. Hu, (2024), [arXiv:2405.02168 \[astro-ph.CO\]](#).
  - [12] D. Shlivko and P. J. Steinhardt, *Phys. Lett. B* **855**, 138826 (2024), [arXiv:2405.03933 \[astro-ph.CO\]](#).
  - [13] B. R. Dinda, *JCAP* **09**, 062 (2024), [arXiv:2405.06618 \[astro-ph.CO\]](#).
  - [14] O. Seto and Y. Toda, *Phys. Rev. D* **110**, 083501 (2024), [arXiv:2405.11869 \[astro-ph.CO\]](#).
  - [15] N. Roy, (2024), [arXiv:2406.00634 \[astro-ph.CO\]](#).
  - [16] I. D. Gialamas, G. Hütsi, K. Kannike, A. Racioppi, M. Raidal, M. Vasar, and H. Veermäe, (2024), [arXiv:2406.07533 \[astro-ph.CO\]](#).

- [17] Y. Toda, W. Giarè, E. Özülker, E. Di Valentino, and S. Vagnozzi, *Phys. Dark Univ.* **46**, 101676 (2024), [arXiv:2407.01173 \[astro-ph.CO\]](#).
- [18] H. Wang, Z.-Y. Peng, and Y.-S. Piao, (2024), [arXiv:2406.03395 \[astro-ph.CO\]](#).
- [19] L. Orchard and V. H. Cárdenas, (2024), [arXiv:2407.05579 \[astro-ph.CO\]](#).
- [20] H. Wang, G. Ye, and Y.-S. Piao, (2024), [arXiv:2407.11263 \[astro-ph.CO\]](#).
- [21] W. Giarè, M. Najafi, S. Pan, E. Di Valentino, and J. T. Firouzjaee, (2024), [arXiv:2407.16689 \[astro-ph.CO\]](#).
- [22] J.-Q. Jiang, W. Giarè, S. Gariazzo, M. G. Dainotti, E. Di Valentino, O. Mena, D. Pedrotti, S. S. da Costa, and S. Vagnozzi, (2024), [arXiv:2407.18047 \[astro-ph.CO\]](#).
- [23] J.-Q. Jiang, D. Pedrotti, S. S. da Costa, and S. Vagnozzi, (2024), [arXiv:2408.02365 \[astro-ph.CO\]](#).
- [24] B. R. Dinda and R. Maartens, (2024), [arXiv:2407.17252 \[astro-ph.CO\]](#).
- [25] A. C. Alfano, O. Luongo, and M. Muccino, *JCAP* **12**, 055 (2024), [arXiv:2408.02536 \[astro-ph.CO\]](#).
- [26] B. Ghosh and C. Bengaly, *Phys. Dark Univ.* **46**, 101699 (2024), [arXiv:2408.04432 \[astro-ph.CO\]](#).
- [27] D. Pedrotti, J.-Q. Jiang, L. A. Escamilla, S. S. da Costa, and S. Vagnozzi, *Phys. Rev. D* **111**, 023506 (2025), [arXiv:2408.04530 \[astro-ph.CO\]](#).
- [28] Y.-H. Pang, X. Zhang, and Q.-G. Huang, (2024), [arXiv:2408.14787 \[astro-ph.CO\]](#).
- [29] S. Roy Choudhury and T. Okumura, *Astrophys. J. Lett.* **976**, L11 (2024), [arXiv:2409.13022 \[astro-ph.CO\]](#).
- [30] W. Giarè, (2024), [arXiv:2409.17074 \[astro-ph.CO\]](#).
- [31] H. Wang, G. Ye, J.-Q. Jiang, and Y.-S. Piao, (2024), [arXiv:2409.17879 \[astro-ph.CO\]](#).
- [32] C.-G. Park, J. de Cruz Perez, and B. Ratra, (2024), [arXiv:2410.13627 \[astro-ph.CO\]](#).
- [33] E. Specogna, W. Giarè, and E. Di Valentino, (2024), [arXiv:2411.03896 \[astro-ph.CO\]](#).
- [34] Y.-H. Pang, X. Zhang, and Q.-G. Huang, (2024), [arXiv:2411.14189 \[astro-ph.CO\]](#).
- [35] K. V. Berghaus, J. A. Kable, and V. Miranda, (2024), [arXiv:2404.14341 \[astro-ph.CO\]](#).
- [36] W. Giarè, M. A. Sabogal, R. C. Nunes, and E. Di Valentino, (2024), [arXiv:2404.15232 \[astro-ph.CO\]](#).
- [37] C. Escamilla-Rivera and R. Sandoval-Orozco, *JHEAp* **42**, 217 (2024), [arXiv:2405.00608 \[astro-ph.CO\]](#).

- [38] S. Bhattacharya, G. Borghetto, A. Malhotra, S. Parameswaran, G. Tasinato, and I. Zavala, *JCAP* **09**, 073 (2024), [arXiv:2405.17396 \[astro-ph.CO\]](#).
- [39] J. J. Heckman, O. F. Ramadan, and J. Sakstein, *Phys. Rev. D* **111**, 023510 (2025), [arXiv:2406.04408 \[astro-ph.CO\]](#).
- [40] A. Chudaykin and M. Kunz, (2024), [arXiv:2407.02558 \[astro-ph.CO\]](#).
- [41] G.-H. Du, P.-J. Wu, T.-N. Li, and X. Zhang, (2024), [arXiv:2407.15640 \[astro-ph.CO\]](#).
- [42] T.-N. Li, P.-J. Wu, G.-H. Du, S.-J. Jin, H.-L. Li, J.-F. Zhang, and X. Zhang, (2024), [arXiv:2407.14934 \[astro-ph.CO\]](#).
- [43] G. Ye, M. Martinelli, B. Hu, and A. Silvestri, (2024), [arXiv:2407.15832 \[astro-ph.CO\]](#).
- [44] S. Sohail, S. Alam, S. Akthar, and M. W. Hossain, (2024), [arXiv:2408.03229 \[astro-ph.CO\]](#).
- [45] W. J. Wolf, C. García-García, D. J. Bartlett, and P. G. Ferreira, (2024), [arXiv:2408.17318 \[astro-ph.CO\]](#).
- [46] W. J. Wolf, P. G. Ferreira, and C. García-García, (2024), [arXiv:2409.17019 \[astro-ph.CO\]](#).
- [47] G. Alestas, M. Caldarola, S. Kuroyanagi, and S. Nesseris, (2024), [arXiv:2410.00827 \[astro-ph.CO\]](#).
- [48] S. Bhattacharya, G. Borghetto, A. Malhotra, S. Parameswaran, G. Tasinato, and I. Zavala, (2024), [arXiv:2410.21243 \[astro-ph.CO\]](#).
- [49] G. Ye, (2024), [arXiv:2411.11743 \[astro-ph.CO\]](#).
- [50] T.-N. Li, Y.-H. Li, G.-H. Du, P.-J. Wu, L. Feng, J.-F. Zhang, and X. Zhang, (2024), [arXiv:2411.08639 \[astro-ph.CO\]](#).
- [51] S. Akthar and M. W. Hossain, (2024), [arXiv:2411.15892 \[astro-ph.CO\]](#).
- [52] S. S. da Costa, *Phys. Dark Univ.* **47**, 101791 (2025), [arXiv:2412.14290 \[astro-ph.CO\]](#).
- [53] G.-H. Du, T.-N. Li, P.-J. Wu, L. Feng, S.-H. Zhou, J.-F. Zhang, and X. Zhang, (2025), [arXiv:2501.10785 \[astro-ph.CO\]](#).
- [54] W. J. Wolf and P. G. Ferreira, *Phys. Rev. D* **108**, 103519 (2023), [arXiv:2310.07482 \[astro-ph.CO\]](#).
- [55] A. G. Adame *et al.* (DESI), (2024), [arXiv:2411.12022 \[astro-ph.CO\]](#).
- [56] E. Calabrese, A. Slosar, A. Melchiorri, G. F. Smoot, and O. Zahn, *Phys. Rev. D* **77**, 123531 (2008), [arXiv:0803.2309 \[astro-ph\]](#).
- [57] N. Aghanim *et al.* (Planck), *Astron. Astrophys.* **641**, A6 (2020), [Erratum: *Astron. Astrophys.* 652, C4 (2021)], [arXiv:1807.06209 \[astro-ph.CO\]](#).

- [58] C.-G. Park and B. Ratra, (2025), [arXiv:2501.03480 \[astro-ph.CO\]](#).
- [59] Y. Akrami *et al.* (Planck), *Astron. Astrophys.* **643**, A42 (2020), [arXiv:2007.04997 \[astro-ph.CO\]](#).
- [60] E. Rosenberg, S. Gratton, and G. Efstathiou, *Mon. Not. Roy. Astron. Soc.* **517**, 4620 (2022), [arXiv:2205.10869 \[astro-ph.CO\]](#).
- [61] M. Tristram *et al.*, *Astron. Astrophys.* **682**, A37 (2024), [arXiv:2309.10034 \[astro-ph.CO\]](#).
- [62] M. Ishak *et al.* (DESI), (2024), [arXiv:2411.12026 \[astro-ph.CO\]](#).
- [63] I. J. Allali and A. Notari, (2024), [arXiv:2406.14554 \[astro-ph.CO\]](#).
- [64] S. Aiola *et al.* (ACT), *JCAP* **12**, 047 (2020), [arXiv:2007.07288 \[astro-ph.CO\]](#).
- [65] D. Dutcher *et al.* (SPT-3G), *Phys. Rev. D* **104**, 022003 (2021), [arXiv:2101.01684 \[astro-ph.CO\]](#).
- [66] L. Balkenhol *et al.* (SPT-3G), *Phys. Rev. D* **108**, 023510 (2023), [arXiv:2212.05642 \[astro-ph.CO\]](#).
- [67] F. Beutler, C. Blake, M. Colless, D. H. Jones, L. Staveley-Smith, G. B. Poole, L. Campbell, Q. Parker, W. Saunders, and F. Watson, *Mon. Not. Roy. Astron. Soc.* **423**, 3430 (2012), [arXiv:1204.4725 \[astro-ph.CO\]](#).
- [68] A. J. Ross, L. Samushia, C. Howlett, W. J. Percival, A. Burden, and M. Manera, *Mon. Not. Roy. Astron. Soc.* **449**, 835 (2015), [arXiv:1409.3242 \[astro-ph.CO\]](#).
- [69] S. Alam *et al.* (BOSS), *Mon. Not. Roy. Astron. Soc.* **470**, 2617 (2017), [arXiv:1607.03155 \[astro-ph.CO\]](#).
- [70] S. Alam *et al.* (eBOSS), *Phys. Rev. D* **103**, 083533 (2021), [arXiv:2007.08991 \[astro-ph.CO\]](#).
- [71] N. Aghanim *et al.* (Planck), *Astron. Astrophys.* **641**, A5 (2020), [arXiv:1907.12875 \[astro-ph.CO\]](#).
- [72] M. Tristram *et al.*, *Astron. Astrophys.* **647**, A128 (2021), [arXiv:2010.01139 \[astro-ph.CO\]](#).
- [73] J. Carron, M. Mirmelstein, and A. Lewis, *JCAP* **09**, 039 (2022), [arXiv:2206.07773 \[astro-ph.CO\]](#).
- [74] M. S. Madhavacheril *et al.* (ACT), *Astrophys. J.* **962**, 113 (2024), [arXiv:2304.05203 \[astro-ph.CO\]](#).
- [75] F. J. Qu *et al.* (ACT), *Astrophys. J.* **962**, 112 (2024), [arXiv:2304.05202 \[astro-ph.CO\]](#).
- [76] D. Scolnic *et al.*, *Astrophys. J.* **938**, 113 (2022), [arXiv:2112.03863 \[astro-ph.CO\]](#).
- [77] J. Torrado and A. Lewis, *JCAP* **05**, 057 (2021), [arXiv:2005.05290 \[astro-ph.IM\]](#).



- [78] D. Blas, J. Lesgourgues, and T. Tram, *JCAP* **1107**, 034 (2011), [arXiv:1104.2933 \[astro-ph.CO\]](#).
- [79] A. Gelman and D. B. Rubin, *Statist. Sci.* **7**, 457 (1992).
- [80] E. B. Holm, A. Nygaard, J. Dakin, S. Hannestad, and T. Tram, (2023), [arXiv:2312.02972 \[astro-ph.CO\]](#).
- [81] H. Akaike, *IEEE Trans. Automatic Control* **19**, 716 (1974).
- [82] S. Dodelson and F. Schmidt, *Modern Cosmology* (2020).
- [83] D. Green and J. Meyers, (2024), [arXiv:2407.07878 \[astro-ph.CO\]](#).
- [84] M. Loverde and Z. J. Weiner, (2024), [arXiv:2410.00090 \[astro-ph.CO\]](#).
- [85] Y. Akrami *et al.* (Planck), *Astron. Astrophys.* **641**, A10 (2020), [arXiv:1807.06211 \[astro-ph.CO\]](#).
- [86] G. Ye and Y.-S. Piao, *Phys. Rev. D* **101**, 083507 (2020), [arXiv:2001.02451 \[astro-ph.CO\]](#).
- [87] G. Ye, B. Hu, and Y.-S. Piao, *Phys. Rev. D* **104**, 063510 (2021), [arXiv:2103.09729 \[astro-ph.CO\]](#).
- [88] J.-Q. Jiang and Y.-S. Piao, *Phys. Rev. D* **105**, 103514 (2022), [arXiv:2202.13379 \[astro-ph.CO\]](#).
- [89] T. L. Smith, M. Lucca, V. Poulin, G. F. Abellan, L. Balkenhol, K. Benabed, S. Galli, and R. Murgia, *Phys. Rev. D* **106**, 043526 (2022), [arXiv:2202.09379 \[astro-ph.CO\]](#).
- [90] J.-Q. Jiang, G. Ye, and Y.-S. Piao, *Mon. Not. Roy. Astron. Soc.* **527**, L54 (2023), [arXiv:2210.06125 \[astro-ph.CO\]](#).
- [91] Z.-Y. Peng and Y.-S. Piao, *Phys. Rev. D* **109**, 023519 (2024), [arXiv:2308.01012 \[astro-ph.CO\]](#).
- [92] J.-Q. Jiang and Y.-S. Piao, (2025), [arXiv:2501.16883 \[astro-ph.CO\]](#).
- [93] E. Di Valentino, A. Melchiorri, Y. Fantaye, and A. Heavens, *Phys. Rev. D* **98**, 063508 (2018), [arXiv:1808.09201 \[astro-ph.CO\]](#).
- [94] W. Giarè, F. Renzi, O. Mena, E. Di Valentino, and A. Melchiorri, *Mon. Not. Roy. Astron. Soc.* **521**, 2911 (2023), [arXiv:2210.09018 \[astro-ph.CO\]](#).
- [95] R. Kallosh and A. Linde, *Phys. Rev. D* **106**, 023522 (2022), [arXiv:2204.02425 \[hep-th\]](#).
- [96] M. Braglia, W. T. Emond, F. Finelli, A. E. Gumrukcuoglu, and K. Koyama, *Phys. Rev. D* **102**, 083513 (2020), [arXiv:2005.14053 \[astro-ph.CO\]](#).
- [97] G. Ye, J.-Q. Jiang, and Y.-S. Piao, *Phys. Rev. D* **106**, 103528 (2022), [arXiv:2205.02478 \[astro-ph.CO\]](#).

- [98] J.-Q. Jiang, G. Ye, and Y.-S. Piao, *Phys. Lett. B* **851**, 138588 (2024), [arXiv:2303.12345 \[astro-ph.CO\]](#).
- [99] M. Braglia, A. Linde, R. Kallosh, and F. Finelli, *JCAP* **04**, 033 (2023), [arXiv:2211.14262 \[astro-ph.CO\]](#).
- [100] G. D’Amico, N. Kaloper, and A. Westphal, *Phys. Rev. D* **105**, 103527 (2022), [arXiv:2112.13861 \[hep-th\]](#).
- [101] W. Giarè, S. Pan, E. Di Valentino, W. Yang, J. de Haro, and A. Melchiorri, *JCAP* **09**, 019 (2023), [arXiv:2305.15378 \[astro-ph.CO\]](#).
- [102] C. Fu and S.-J. Wang, *Phys. Rev. D* **109**, L041304 (2024), [arXiv:2310.12932 \[astro-ph.CO\]](#).
- [103] W. Giarè, *Phys. Rev. D* **109**, 123545 (2024), [arXiv:2404.12779 \[astro-ph.CO\]](#).
- [104] L. Knox and M. Millea, *Phys. Rev. D* **101**, 043533 (2020), [arXiv:1908.03663 \[astro-ph.CO\]](#).
- [105] L. Perivolaropoulos and F. Skara, *New Astron. Rev.* **95**, 101659 (2022), [arXiv:2105.05208 \[astro-ph.CO\]](#).
- [106] E. Di Valentino, O. Mena, S. Pan, L. Visinelli, W. Yang, A. Melchiorri, D. F. Mota, A. G. Riess, and J. Silk, *Class. Quant. Grav.* **38**, 153001 (2021), [arXiv:2103.01183 \[astro-ph.CO\]](#).
- [107] S. Vagnozzi, *Universe* **9**, 393 (2023), [arXiv:2308.16628 \[astro-ph.CO\]](#).
- [108] T. M. C. Abbott *et al.* (DES), *Astrophys. J. Lett.* **973**, L14 (2024), [arXiv:2401.02929 \[astro-ph.CO\]](#).
- [109] G. Efstathiou, (2024), [arXiv:2408.07175 \[astro-ph.CO\]](#).

## Appendix A: Results of Relevant Parameters

Parameter	Plik	CamSpec	HiLLiPoP
$H_0$	$67.95(67.91) \pm 0.39$	$67.74(67.82) \pm 0.37$	$67.95(67.82) \pm 0.38$
$100\omega_b$	$2.246(2.246) \pm 0.013$	$2.226(2.231) \pm 0.013$	$2.231(2.231) \pm 0.012$
$\omega_{\text{cdm}}$	$0.11866(0.11876) \pm 0.00084$	$0.11858(0.11847) \pm 0.00081$	$0.11816(0.11856) \pm 0.00084$
$10^9 A_s$	$2.117(2.111)_{-0.029}^{+0.026}$	$2.108(2.106)_{-0.029}^{+0.025}$	$2.120(2.111) \pm 0.023$
$n_s$	$0.9683(0.9689) \pm 0.0036$	$0.9663(0.9657) \pm 0.0036$	$0.9696(0.9698) \pm 0.0035$
$\tau_{\text{reio}}$	$0.0587(0.0570)_{-0.0075}^{+0.0067}$	$0.0575(0.0559) \pm 0.0072$	$0.0615(0.0586) \pm 0.0061$
$\chi^2$	4203.50	12404.05	31994.57

TABLE V. The mean (best-fit)  $\pm 1\sigma$  errors of relevant parameters and  $\chi^2$  values for  $\Lambda$ CDM model. The datasets are Planck PR3 and PR4 likelihoods, respectively combined with DESI BAO, CMB lensing, and Pantheon+.

Parameter	Plik	CamSpec	HiLLiPoP
$w_0$	$-0.831(-0.826) \pm 0.063$	$-0.832(-0.838) \pm 0.063$	$-0.842(-0.856) \pm 0.063$
$w_a$	$-0.73(-0.73)_{-0.25}^{+0.29}$	$-0.73(-0.72)_{-0.25}^{+0.29}$	$-0.64(-0.54)_{-0.24}^{+0.30}$
$H_0$	$68.05(67.97) \pm 0.72$	$67.90(67.94) \pm 0.72$	$67.89(67.78) \pm 0.71$
$100\omega_b$	$2.240(2.240) \pm 0.014$	$2.220(2.215) \pm 0.014$	$2.226(2.227) \pm 0.013$
$\omega_{\text{cdm}}$	$0.11950(0.11943) \pm 0.00099$	$0.11944(0.11956) \pm 0.00096$	$0.11880(0.11844) \pm 0.00098$
$10^9 A_s$	$2.098(2.098) \pm 0.028$	$2.088(2.081) \pm 0.028$	$2.107(2.117) \pm 0.024$
$n_s$	$0.9661(0.9661) \pm 0.0038$	$0.9641(0.9631) \pm 0.0038$	$0.9681(0.9696) \pm 0.0037$
$\tau_{\text{reio}}$	$0.0544(0.0542) \pm 0.0073$	$0.0530(0.0510) \pm 0.0072$	$0.0592(0.0614) \pm 0.0061$
$\chi^2$	4195.93	12396.23	31988.66

TABLE VI. The mean (best-fit)  $\pm 1\sigma$  errors of relevant parameters and  $\chi^2$  values for  $w_0 w_a$ CDM model. The datasets are Planck PR3 and PR4 likelihoods, respectively combined with DESI BAO, CMB lensing, and Pantheon+.

Parameter	Plik	CamSpec	HiLLiPoP
$A_L$	$1.083(1.095)^{+0.033}_{-0.037}$	$1.075(1.072) \pm 0.034$	$1.062(1.064) \pm 0.035$
$n_s$	$0.9707(0.9711) \pm 0.0037$	$0.9687(0.9672) \pm 0.0038$	$0.9716(0.9732) \pm 0.0034$
$H_0$	$68.39(68.42) \pm 0.43$	$68.15(68.08) \pm 0.40$	$68.26(68.46) \pm 0.39$
$100\omega_b$	$2.254(2.251) \pm 0.014$	$2.235(2.233)^{+0.013}_{-0.012}$	$2.237(2.243)^{+0.012}_{-0.011}$
$\omega_{\text{cdm}}$	$0.11767(0.11760) \pm 0.00093$	$0.11770(0.11784) \pm 0.00088$	$0.11748(0.11719) \pm 0.00087$
$\tau_{\text{reio}}$	$0.0495(0.0514)^{+0.0085}_{-0.0075}$	$0.0492(0.0493) \pm 0.0083$	$0.0578(0.0604) \pm 0.0062$
$10^9 A_s$	$2.061(2.059) \pm 0.037$	$2.059(2.057) \pm 0.035$	$2.085(2.093) \pm 0.030$
$\chi^2$	4197.28	12399.81	31991.93

TABLE VII. The mean (best-fit)  $\pm 1\sigma$  errors of relevant parameters and  $\chi^2$  values for  $\Lambda\text{CDM}+A_L$  model. The datasets are Planck PR3 and PR4 likelihoods, respectively combined with DESI BAO, CMB lensing, and Pantheon+.

Parameter	Plik	CamSpec	HiLLiPoP
$A_L$	$1.066(1.071) \pm 0.041$	$1.051(1.050) \pm 0.040$	$1.043(1.037) \pm 0.040$
$w_0$	$-0.859(-0.862) \pm 0.063$	$-0.851(-0.866) \pm 0.064$	$-0.859(-0.856) \pm 0.064$
$w_a$	$-0.51(-0.45)^{+0.32}_{-0.25}$	$-0.58(-0.48)^{+0.32}_{-0.26}$	$-0.52(-0.57)^{+0.30}_{-0.26}$
$H_0$	$67.92(67.76) \pm 0.73$	$67.84(67.71) \pm 0.73$	$67.81(68.20) \pm 0.71$
$100\omega_b$	$2.250(2.252) \pm 0.015$	$2.229(2.231)^{+0.016}_{-0.014}$	$2.233(2.237)^{+0.014}_{-0.013}$
$\omega_{\text{cdm}}$	$0.1182(0.1180) \pm 0.0013$	$0.1184(0.1183) \pm 0.0012$	$0.1180(0.1180) \pm 0.0012$
$10^9 A_s$	$2.062(2.068)^{+0.037}_{-0.033}$	$2.061(2.067)^{+0.037}_{-0.032}$	$2.088(2.092) \pm 0.030$
$n_s$	$0.9695(0.9704) \pm 0.0044$	$0.9669(0.9662) \pm 0.0043$	$0.9700(0.9715) \pm 0.0041$
$\tau_{\text{reio}}$	$0.0491(0.0520)^{+0.0086}_{-0.0075}$	$0.0489(0.0504)^{+0.0087}_{-0.0072}$	$0.0577(0.0581) \pm 0.0062$
$\chi^2$	4192.24	12394.64	31986.84

TABLE VIII. The mean (best-fit)  $\pm 1\sigma$  errors of relevant parameters and  $\chi^2$  values for  $w_0w_a\text{CDM}+A_L$  model. The datasets are Planck PR3 and PR4 likelihoods, respectively combined with DESI BAO, CMB lensing, and Pantheon+.

Parameter	Plik	CamSpec	HiLLiPoP
$A_L$	$1.062 \pm 0.035$	$1.054 \pm 0.034$	$1.042 \pm 0.035$
$H_0$	$67.84 \pm 0.44$	$67.62 \pm 0.43$	$67.74 \pm 0.43$
$100\omega_b$	$2.245 \pm 0.014$	$2.226 \pm 0.014$	$2.228 \pm 0.013$
$\omega_{\text{cdm}}$	$0.11887 \pm 0.00097$	$0.11886 \pm 0.00093$	$0.11860 \pm 0.00094$
$10^9 A_s$	$2.065^{+0.037}_{-0.032}$	$2.062^{+0.036}_{-0.032}$	$2.088 \pm 0.030$
$n_s$	$0.9676 \pm 0.0038$	$0.9657 \pm 0.0038$	$0.9686 \pm 0.0036$
$\tau_{\text{reio}}$	$0.0489^{+0.0086}_{-0.0074}$	$0.0485^{+0.0083}_{-0.0072}$	$0.0571 \pm 0.0062$

TABLE IX. The mean  $\pm 1\sigma$  errors of relevant parameters for  $\Lambda\text{CDM}+A_L$  model. The datasets are Planck PR3 and PR4 likelihoods, respectively combined with pre-DESI BAO, CMB lensing, and Pantheon+.

Parameter	Plik	CamSpec	HiLLiPoP
$A_L$	$1.067 \pm 0.044$	$1.052 \pm 0.041$	$1.046 \pm 0.042$
$w_0$	$-0.906 \pm 0.062$	$-0.902 \pm 0.063$	$-0.905 \pm 0.062$
$w_a$	$-0.25^{+0.29}_{-0.23}$	$-0.30^{+0.29}_{-0.24}$	$-0.26^{+0.28}_{-0.23}$
$H_0$	$67.16 \pm 0.69$	$67.06 \pm 0.68$	$67.07 \pm 0.68$
$100\omega_b$	$2.248 \pm 0.016$	$2.227^{+0.017}_{-0.015}$	$2.231^{+0.016}_{-0.013}$
$\omega_{\text{cdm}}$	$0.1185 \pm 0.0014$	$0.1187 \pm 0.0013$	$0.1183^{+0.0012}_{-0.0013}$
$10^9 A_s$	$2.063 \pm 0.036$	$2.062^{+0.035}_{-0.032}$	$2.087 \pm 0.030$
$n_s$	$0.9686 \pm 0.0047$	$0.9661 \pm 0.0046$	$0.9694 \pm 0.0042$
$\tau_{\text{reio}}$	$0.0488^{+0.0084}_{-0.0075}$	$0.0487^{+0.0082}_{-0.0072}$	$0.0572 \pm 0.0063$

TABLE X. The mean  $\pm 1\sigma$  errors of relevant parameters for  $w_0w_a\text{CDM}+A_L$  model. The datasets are Planck PR3 and PR4 likelihoods, respectively combined with pre-DESI BAO, CMB lensing, and Pantheon+.